2011. Proceedings of the Indiana Academy of Science 120(1-2):104–112

ON THE DETECTION OF DENDRITIC CURRENTS USING FUNCTIONAL MAGNETIC RESONANCE IMAGING

William I. Jay and **Ranjith S. Wijesinghe**: Dept of Physics and Astronomy, Ball State University, Muncie, IN, 47306 USA

ABSTRACT. The currents associated with neuronal activity generate their own magnetic fields which potentially cause a measurable phase change in a magnetic resonance (MR) signal. The feasibility of directly measuring neuronal currents is still under debate. In this paper we model individual dendrites as magnetic current dipoles on a variable lattice structure in order to calculate the magnetic fields and phase shifts generated by active neuronal tissue. Our results show the field produced by an ensemble of simultaneously active dendrites may produce effects measurable using current MRI technology.

Keywords: MRI, phase shift, dendrite, brain, dipole

INTRODUCTION

Magnetic resonance imaging.—Over the past several decades great strides have been made with magnetic resonance imaging (MRI). This powerful technology exploits the intrinsic magnetic properties of matter on the atomic scale to probe materials noninvasively. Although the use of MRI is not limited to the medical fields, that is where it is perhaps most well known. Armed with the excellent spatial resolution provided by MRI, researchers have been able to provide many key insights into the structure and functioning of the brain. In the pursuit of this goal, functional MRI (fMRI) was developed to detect brain activity itself instead of examining solely structural features. Functional magnetic resonance works by detecting a so-called blood oxygenation level-dependent (BOLD) signal (Ogawa 1990). The physical basis for this signal is the fact the hemoglobin contained in red blood cells possesses different magnetic properties depending on whether or not it is oxygenated. However, the BOLD signal does not directly measure neural activity; instead, it is an indirect marker of perfusion and the signature of the metabolic processes of the brain (Heuttel et al. 2009).

Direct detection of neuronal activity.—Direct detection of the magnetic fields from neuronal currents themselves would provide a signal that closely follows the spatial and especially the temporal distribution of neural activity. Direct neuronal mapping through fMRI would give a noninvasive method for mapping the brain's neural pathways (Kwong et al. 1992). This capability would offer a number of immediate benefits:

1) It would allow direct measurements of nerve conduction velocities, an invaluable parameter for neurosurgeons wishing to determine the severity of damaged nerve bundles noninvasively.
2) It could allow for the diagnosis of diseases of the brain when in their preliminary stages. Important examples of these include Multiple Sclerosis, Parkinson's disease, and Alzheimer's.
3) It could facilitate an improved understanding of the ways in which drugs are delivered to the brain as well as the rest of the body.
4) It could provide new insights into the study of chronic pain.
5) It could aid in studies of cognitive function.

Scientific work to date.—Many researchers have tried to detect neuronal currents using MRI (Bodurka and Bandettini 2002; Cassara et al. 2008; Hagberg et al. 2006; Johnston et al. 1996; Kamei et al. 1999; Paley et al. 2009; Troung and Song 2006). However, the feasibility of such studies is still under debate (Konn

Contact: Ranjith S. Wijesinghe, Dept of Physics and Astronomy, Ball State University, Muncie, IN47306 USA765-285-8811 (e-mail: rswijesinghe@bsu.edu).

et al. 2003; Xue et al. 2009). Some studies in the past have attempted to calculate the magnetic fields from action currents and other neural activity from first principles (Cassara et al. 2008; Paley et al 2009). Furthermore, a large body of research exists in the literature in which the magnetic fields from nerves, muscles, and single axons have been evaluated numerically (Swinney & Wikswo 1980; van Egeraat & Wikswo 1993; Woosley et al. 1985). Experimental work has also measured these fields using ferrite-core, wound-wire toroids (Gielen et al. 1986, 1991; Roth & Wikswo 1985; van Egeraat et al. 1990, 1993; Wijesinghe et al. 1991; Wikswo et al. 1980, 1990, 1991). Various investigations also present the results obtained from water phantoms (a type of experimental model), bloodless turtle brains, humans, rat brains, and theoretical calculations (Bandettini et al. 1992; Bodurka et al. 1999; Cassara et al. 2008, Kraus et al. 2008). Some of these studies claim to find measurably large magnetic fields and MRI phase and signal changes generated within the brain (Bodurka & Bandettini 2002; Park & Lee 2007; Xue et al. 2009). Others maintain that the resultant field intensity from human brain activity is simply too weak to detect a meaningful signal in MRI experiments (Chu et al. 2004; Xue et al. 2009). A proposed threshold for the minimum detectable field is on the order of 0.1 nT, corresponding to a minimum phase shift of approximately 0.0002 radians over a voxel (Bandettini et al. 2005). Our goal in this paper is to use calculated magnetic signals generated by dendrite currents in order to estimate the changes in an MRI signal.

METHODS

The dipole model.—From the standpoint of physically modeling the magnetic fields of complex biological systems, one must choose some current distribution to generate the magnetic field. A popular approach (Kaufman et al. 1991; Konn et al. 2003), and one that we continue in this investigation, models magnetic field sources as current dipoles. Past studies have used this method to model large portions of the brain using tens to hundreds of dipoles. Our study expands on this by modeling individual dendrites as magnetic current dipoles. It is also worth noting that the magnetic field from an arbitrary current distribution may be represented as what is known as a multipole expansion (Jackson 1999). In this expansion, the dominating contribution generally comes from the leading dipole term. It is only in the case of special symmetries that higher-order terms deliver large effects, and these special symmetries are not expected to be present in the brain.

The mathematics of the model.—In this model we use the well-known quasi-static approximation of Maxwell's equations. Although the brain can hardly be called a static system, dynamic changes occur at frequencies well below those required for the use of the full machinery of Maxwell's dynamic theory. Generally speaking, the quasi-static approximation is appropriate whenever velocities are much less than the speed of light ($v/c << 1$), a condition satisfied by the brain. Therefore the magnetic field, **B**, generated by an arbitrary current distribution may be given by the Biot-Savart law:

$$\vec{B} = \int \frac{\mu}{4\pi} \frac{I \, d\overrightarrow{l'} \times \vec{r}}{r^3}. \quad (1)$$

In the above equation μ is the magnetic permeability, I is the current, ***dl'*** is the differential length element, and r is the vector distance from the source point to the field point; the primed length element indicates that the integration is to be carried out over the source distribution.

For the case of a magnetic current dipole, the integration may be evaluated to yield the following formula:

$$\vec{B} = \frac{\mu}{4\pi} \frac{\vec{p} \times \vec{R}}{R^3}. \quad (2)$$

Here **p** is the current dipole; **R** is the vector from the dipole at the source point to the field point. In the case of MRI, one is interested in only one Cartesian component of the magnetic field. Without loss of generality, we take this to be the component parallel to the z-axis. For simplicity, we take the field point also to be on the z-axis. These considerations allow us then to write Eq. 2 in the following form with explicit reference to the vector components:

$$B_z = \frac{\mu}{4\pi} \frac{\left(-p_x y' + p_y x'\right)}{\left(z^2 + (x')^2 + (y')^2 + (z')^2 - 2z \cdot z'\right)^{3/2}}. \quad (3)$$

The resultant field from a group of dipoles (i.e. dendrites) will then be a linear superposition of the individual fields given by Eq. 3. Although the brain is a highly nonlinear physical system, the phenomenon of magnetism is linear with

regards to the combination of fields. As such, nonlinearities must introduce themselves within the source distribution and then be transmitted linearly. The effect of nonlinearities is discussed again in our conclusions.

The total resultant field generated by neuronal activity will make a contribution to the phase of the precessing magnetic moments within the sample, which is what MRI actually detects. The phase contribution due to the neuronal magnetic field at a given observation (field) point (x,y,z) in an activated voxel or volume may be calculated via the following equation (Xue et al. 2009):

$$\varphi(x,y,z) = \int_0^{TE} \gamma \cdot B_z(x,y,z,t)dt.$$

In the above equation, TE is the echo time of the MRI echo sequence. γ is the gyromagnetic ratio of the proton, a known value from quantum mechanics of 2.7×10^8 $s^{-1}T^{-1}$ (Wijesinghe & Roth 2009). In our calculations, we approximate this integral by assuming that the dendrites are active for a time less than echo sequence of the MRI, which allows the magnetic field B_z to be taken outside the integral. Thus, the phase shift is approximately the product $\varphi \approx \gamma \cdot B_z \cdot t_{act.}$, where $t_{act.}$ is the activation time of the dendrites, taken to be approximately 0.01 seconds.

Generally speaking, the various magnetic moments in a sample will precess at the so-called Larmor frequency, which depends on the magnitude of the applied magnetic field (for example, by the MRI equipment). From the perspective of the precessing magnetic moments, the biomagnetic field generated by neuronal activity also contributes to the applied magnetic field, thereby altering their precessional frequencies. Thus in this case the phase shift essentially measures the change in the angle between the (precessing) net magnetization before and after neuronal activation.

Model-specific details.—Real macroscopic volumes of human brain tissue are overwhelmingly complex physical systems. Narrowing the focus to relatively small groups of cells or even single cells does not necessarily improve the situation; the complex arborization of dendritic trees have, for example, provided a continual barrier to researchers seeking to understand and model neurons. In this model we are chiefly interested in finding upper bounds on the magnetic field magnitudes and their corresponding phase shifts. The nature of this goal allows us to make a number of simplifying assumptions. We assume: 1.) All the dendrites in the voxel are arranged on a uniform variable lattice structure. 2.) All dendrites are synchronously active. 3.) All dendrites have the same physical properties. 4.) The surrounding medium is homogenous and isotropic.

Dendrite properties: The empirical value for dendrite density in human cortical tissue is on the order of $10^6/mm^3$(Nunez 2006). Our simulations consider the effects of this density as well as several others. The physical dimensions of dendrites vary widely. Apical dendrites may reach lengths of around 300 microns, while the shortest branching dendrites may have lengths of only around 10 microns. A given cortical volume will generally contain more dendrites on the shorter end of the spectrum, and our simulations assume that all dendrites have an average length of 30 microns. Under the assumption that an active dendrite possesses an intracellular current of $\mathbf{I} = 1$ nA (Cassara et al. 2008; Park & Lee 2007), one finds the equivalent current dipole of a dendrite to be:

$$\vec{\mathbf{p}} = \vec{\mathbf{I}} \cdot \mathrm{L} = 3 \times 10^{-5} \text{ nAm}.$$

Spatial properties: As mentioned above, the surrounding medium is taken to be homogenous and isotropic with a magnetic permeability of 1.257×10^{-6} N/A^2. Also, the dendrites are taken to be arranged uniformly on a lattice structure and all to face in a given direction. Although these are both somewhat crude assumptions, they are appropriate given the goal of finding upper bounds for different arrangements. Clearly, the largest fields will be generated by parallel, synchronously active dendrites. Other spatiotemporal distributions would only result in smaller fields. Although these reduced-magnitude fields are perhaps not without interest, they are only of peripheral importance at the moment. Our computer model also has the capability to consider the effects of random dendrite orientations; examples of this are included below.

Computational details.—Our modeling was done independently in Matlab and in Java, with both languages yielding comparable results. Large simulations were carried out on Ball State University's Beowulf supercomputing cluster, a 32-node computer with 64 2.8 GHz Xeon processors. Smaller simulations were carried out on desktop PCs.

Table 1.—Summary of maximum simulated magnetic fields and phase shifts.

	Dendrite Density (dipoles / mm^3)	Maximum B-Field (nT) (Threshold: 0.1 T)	Phase Shift (radians $\times 10^{-3}$) (Threshold: 0.2×10^{-3})
Line (100)	100	0.005	0.082
Layer (10000)	10000	0.24	0.400
Full Voxel	$10^3 = 1000$	0.01	0.021
Full Voxel	$20^3 = 8000$	0.06	0.200
Full Voxel	$30^3 = 9000$	0.19	0.670
Full Voxel	$40^3 = 64{,}000$	0.47	1.600
Full Voxel	$50^3 = 125{,}000$	0.92	3.200
Full Voxel	$60^3 = 216{,}000$	1.60	5.500
Full Voxel	$70^3 = 343{,}000$	2.54	8.800
Full Voxel	$80^3 = 512{,}000$	3.80	13.000
Full Voxel	$90^3 = 729{,}000$	5.41	19.000
Full Voxel	$100^3 = 1{,}000{,}000$	7.43	26.000
Full Voxel	$215^3 = 9\ 938\ 375$	62.1	125.000
Full Voxel (Randomized)	10,000	0.09	0.241
Full Voxel (Randomized)	50,000	0.13	0.348
Full Voxel (Randomized)	100,000	0.41	1.097
Full Voxel (Randomized)	$50^3 = 125{,}000$	0.056	0.150
Full Voxel (Randomized)	1,000,000	0.22	0.589

CALCULATIONS AND RESULTS

In our investigation we conducted a variety of simulations using the model described above. We began by calculating the fields generated by relatively small numbers of dipoles and working up to full-voxel simulations with realistic dendrite densities. The results may be seen in Table 1, with results for randomly oriented dendrites appearing at the bottom.

As one would anticipate, in the case of uniform orientation the maximum simulated magnetic field rose linearly with increasing dendrite density. Because the phase shift given by Eq. 3 is essentially proportional to the magnetic field, the phase shift also rose linearly with increasing dendrite density. Both of these behaviors may be seen clearly in Fig. 1 and Fig. 2, respectively. Fig. 1 and Fig. 2 also display the results of the simulations with random dendrite orientations, and one observes that the magnetic field magnitudes are dramatically smaller.

In order to provide an easier visualization of the field behavior with increasing dendrite density, a cross section of the field was taken from each full-voxel simulation, and they are plotted together in Fig. 3. The cross sections were selected such that they include the fields' extremal values. A three-dimensional representation of the results for two full-voxel simulations may also be seen in Fig. 4 and Fig. 5. Fig. 4 shows the magnetic field at the center of the voxel for the case of 10^6 dendrites. Similarly, Fig. 5 demonstrates the effects of 125,000 randomly oriented dendrites.

DISCUSSION

Taken as a whole, our results demonstrate the low magnitudes associated with the magnetic fields generated by neural activity. In the case of uniform dendrite orientation, the maximum field magnitude approaches and even exceeds the proposed threshold of 0.1 nT at high densities, achieving a value of roughly 7 nT with 10^6 dendrites (see Table 1). In the case of the simulations with randomly oriented dipoles, the results are dramatically smaller (see Table 1 and Fig. 1 & 2), but one observes that many of them are still on the order of the threshold of 0.1 nT proposed by Bandettini. The following section offers interpretation of these results.

CONCLUSIONS AND SUMMARY

The main goal of this project was to construct a theoretical model to describe the magnetic fields generated by active dendrites in human cortical tissue and to assess the feasibility of imaging such activity via MRI. From the results of the simulations above, we report that the magnetic fields generated by dendrites

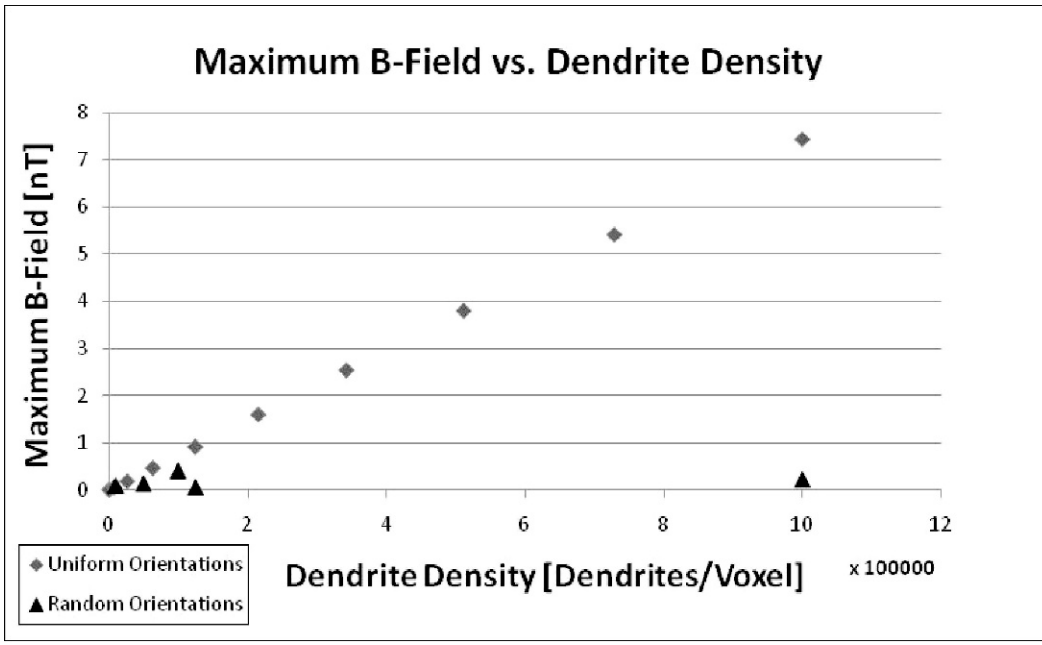

Figure 1.—A plot showing the maximum magnetic field in a simulation versus the dendrite density of the simulation.

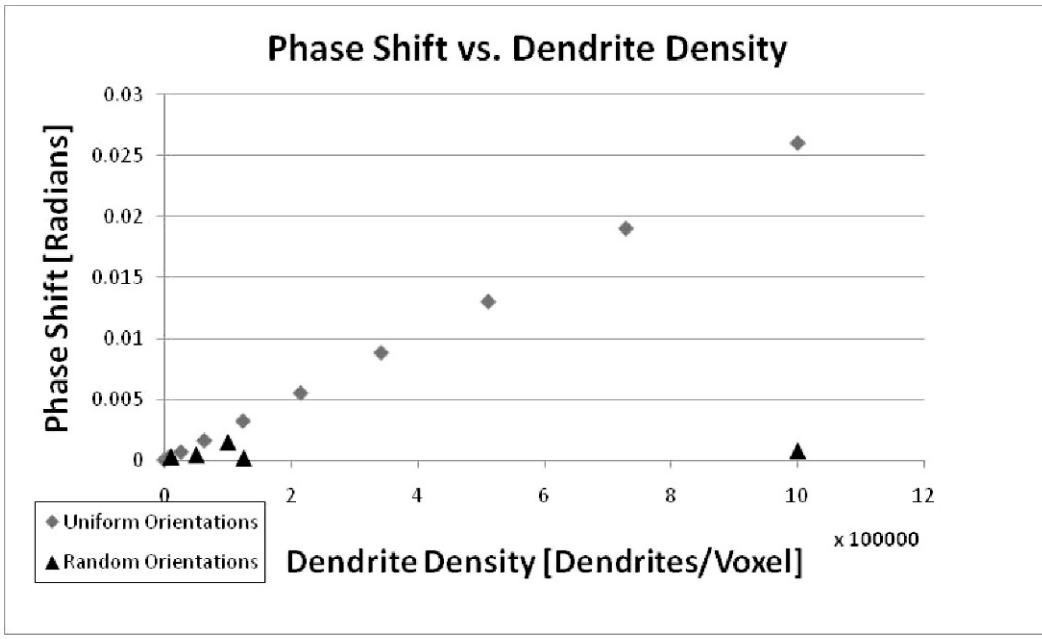

Figure 2.—A plot showing the calculated phase shift in an MR signal versus the dendrite density of the simulation.

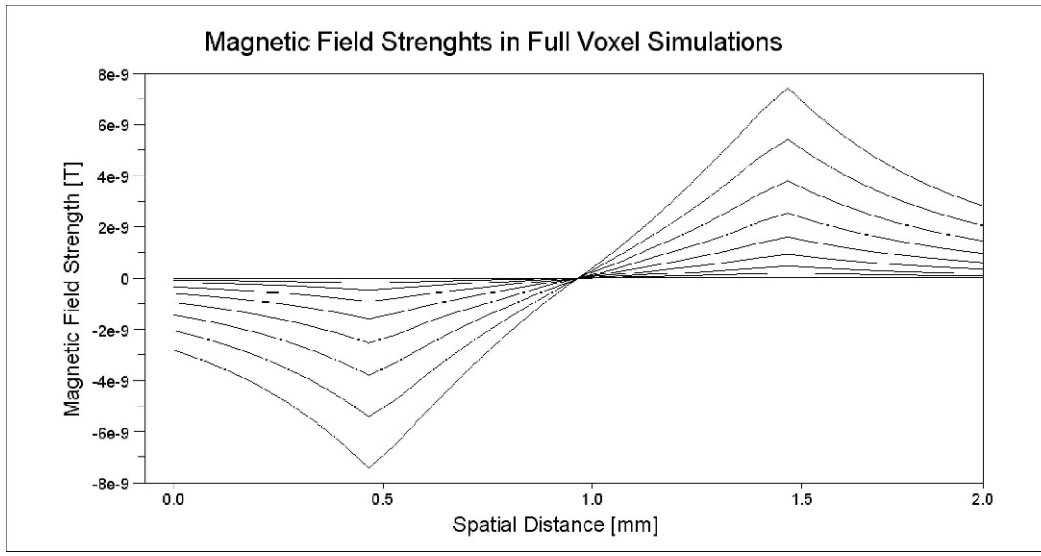

Figure 3.—A plot showing cross sections of the magnetic field in a voxel for the first ten full-voxel simulations given in Table 1. The sharp peaks correspond to the maxima and minima of the fields within the voxels. The sharply pointed top curve corresponds to a dendrite density of 10^6 / mm^3 while the flattest curve corresponds to a dendrite density of 1000 / mm^3.

are potentially measurable using MRI techniques in the near future. Nevertheless, we now address several possible sources of overestimation regarding the fields and phase shifts in our model. 1.) The magnetic field of a dendrite consists of a biphasic signal because of the physical depolarization and repolarization processes. Although the repolarization occurs more slowly than the initial depolarization, it also is weaker, such that the integrated phase shifts from the two nearly cancel. Unless very brief (~ms), precisely-timed pulse sequences are developed, this activity will be very difficult to detect. However, it is possible that such pulse sequences may be developed in the near future. 2.) This model considers the field just outside

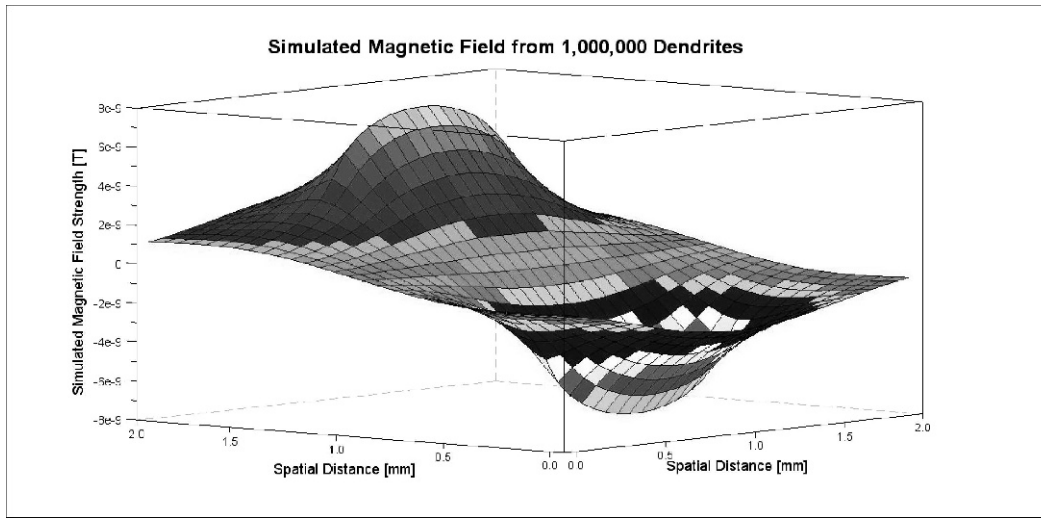

Figure 4.—A three-dimensional plot showing the behavior of the magnetic field at the vertical center of the voxel for the case of 10^6 dendrites / mm^3.

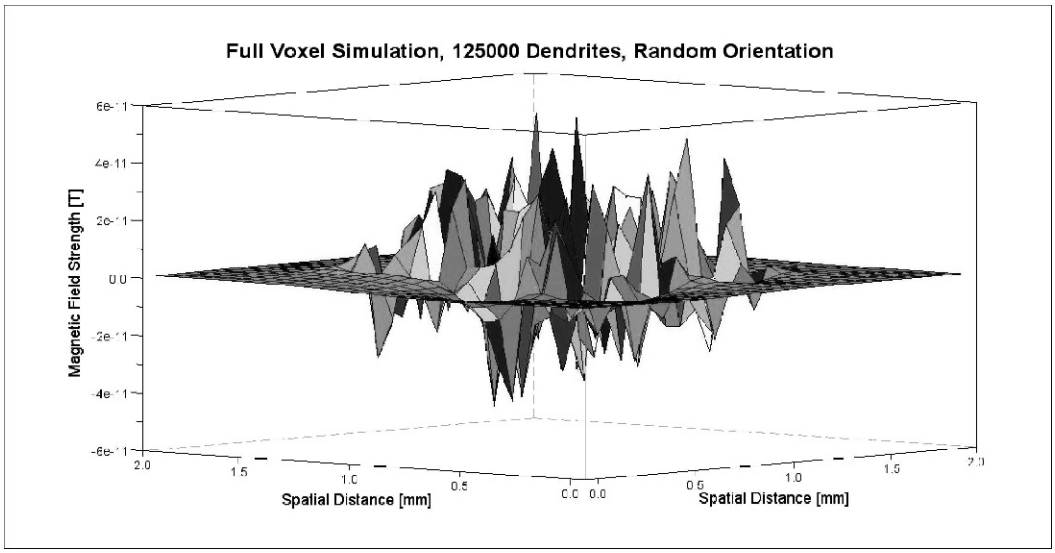

Figure 5.—A three-dimensional plot showing the behavior of the magnetic field at the vertical center of the voxel for the case of 125,000 randomly oriented dendrites. One observes that the maximum field strength is diminished in comparison with the case of parallel orientation given in Table 1.

the dendrites, where it is the largest. Generally speaking, the field will fall off sharply with increasing distance. 3.) Not all dendrites in a realistic voxel will be active simultaneously, suggesting that the lower-density simulations may provide a more accurate description of real tissue. 4.) The currents of the brain will generally not point in the same direction. This complication we have addressed in simulations using random dipole orientations (Table 1 & Fig. 5), which seem to suggest that the fields – in spite of being reduced by at least an order of magnitude – are still on the order of the proposed threshold of 0.1 nT.

Our analysis assumes that the magnetic resonance study is performed using a typical static magnetic field strength on the order of 1 T. As such, the fractional change in magnetic field strength brought about by the neuronal activity is seen to be extremely small, thereby making detection extremely difficult. However, these currents might more easily be measured using ultra-low field MRI systems (Cassara & Maraviglia 2008; Kraus et al. 2008). The capabilities of these systems have yet to be tested on biomagnetic signals. Perhaps the signal-to-noise ratio could be increased by applying a large field to polarize the spins; during the detection phase the large field could then be quickly reduced in order to maximize the fractional field change due to neuronal activity. Clearly, great ingenuity would be required in order to achieve this rapid switching without also introducing confounding effects.

In conclusion, based on our calculations using a dipole model, we are cautiously optimistic about the prospects for direct detection in the future. Researchers in magnetic resonance technology continually develop clever and imaginative new techniques that allow for the solution of previously intractable problems. We hope that our analysis will help clarify the roadblocks on the path to true functional imaging of dendritic and neuronal activity.

ACKNOWLEDGEMENTS

We gratefully acknowledge our support from the Indiana Academy of Science.

REFERENCES

Badettini, P.A., N. Petridou & J. Boduraka. 2005. Direct detection of neuronal activity with MRI: fantasy, possibility, or reality? Applied Magnetic Resonance 29:65–88.

Bandettini, P.A., E.C. Wong, R.S. Hinks, R.S. Tikofsky & J.S. Hyde. 1992. Time course EPI of human brain function during task activation Magnetic Resonance in Medicine 25:390–397.

Bodurka, J. & P.A. Bandettini. 2002. Toward direct mapping of neuronal activity: MRI detection of ultraweak transient magnetic field changes. Magnetic Resonance in Medicine 47:1052–1058.

Bodurka, J., A. Jesmanowicz, J.S. Hyde, H. Xu, L. Estkowski & S.J. Li. 1999. Current-induced magnetic resonance phase imaging. Journal of Magnetic Resonance 137:265–271.

Cassara, A.M., G.E. Hagberg, M. Bianciardi, M. Migliore & B. Maraviglia. 2008. Realistic simulations of neuronal activity: A contribution to the debate on direct detection of neuronal currents by MRI. NeuroImage 39:87–106.

Cassara, A.M. & B. Maraviglia. 2008. Microscopic investigation of the resonant mechanism for the implementation of nc-MRI at ultra-low field MRI. NeuroImage 41:1228–1241.

Chu, R., J. de Zwart, P. van Gelderen, M. Fukunaga, P. Kellman, T. Holroyd & J.H. Duyn. 2004. Hunting for neuronal currents: absence of rapid MRI signal changes during visual-evoked response. Neuroimage 23:1059–1067.

Gielen, F.L.H., B.J. Roth & J.P. Wikswo. 1986. Capabilities of a toroid-amplifier system for magnetic measurement of current in biological tissue. IEEE Transactions on Biomedical Engineering 33:910–921.

Gielen, F.L.H., R.N. Friedman & J.P. Wikswo. 1991. In vivo magnetic and electric recordings from nerve bundles and single motor units in mammalian skeletal muscle. Journal of General Physiology 98:1043–1061.

Hagberg, G.E., M. Bianciardi & B. Maraviglia. 2006. Challenges for detection of neuronal currents by MRI. Magnetic Resonance in Medicine 24: 483–493.

Heuttel, S.A., A.W. Song & G. McCarthy. 2009. Functional Magnetic Resonance Imaging. 2nd ed. Sinauer Associates, Sunderland, MA.

Jackson, J.D. 1999. Classical Electrodynamics. 3rd ed. Wiley, New York.

Johnston, D., J.C. Magee, C.M. Colbert & B.R. Christie. 1996. Active properties of neuronal dendrites. Annual Review of Neuroscience 19: 165–186.

Kamei, H., K. Iramina, K. Yoshlkawa & S. Ueno. 1999. Neuronal current distribution imaging using magnetic resonance. IEEE Transanctions on Magnetics 35:4109–4111.

Kaufman, L., J.H. Kaufman & J.Z. Wang. 1991. On cortical folds and neuromagnetic fields. Electroencephalography and Clinical Neurophysiology 79:211–229.

Konn, D., P. Gowland & R. Bowtell. 2003. MRI detection of weak magnetic fields due to an extended current dipole in a conduction sphere: A model for direct detection of neuronal currents in the brain. Magnetic Resonance in Medicine 50:40–49.

Kraus, R.H., P. Volegov, A. Matlachov & M. Espy. 2008. Toward direct neural current imaging by resonant mechanisms at ultra-low field. Neuroimage. 39:310–317.

Kwong, K., T. Brady & B. Rosen. 1992. Dynamic magnetic resonance imaging of human brain activity during primary sensory stimulation. Proceedings of the National Academy of Science USA 89:5675–5679.

Nunez, P.L. & R. Srinivasan. 2006. Electric Fields of the Brain the Neurophysics of EEG. 2nd ed. Oxford University Press, New York.

Ogawa, S., T.M. Lee, A.R. Kay & D.W. Tank. 1990. Brain magnetic resonance imaging with contrast dependence on blood oxygenation. Proceedings of the National Academy of Science USA. 87:9868–9872.

Paley, M.N.J., L.S. Chow, E.W. Whitby & G.G. Cook. 2009. Modeling of axonal fields in the optic nerve for direct MR detection studies. Image and Vision Computing 27:331–341.

Park, T.S. & S.Y. Lee. 2007. Effects of neuronal magnetic field on MRI: Numerical analysis with axon and dendrite models. NeuroImage 35:531–538.

Roth, B.J. & J.P. Wikswo. 1985. The magnetic field of a single nerve axon: A comparison of theory and experiment. Biophysics Journal 48:93–109.

Swinney, K.R. & J.P. Wikswo. 1980. A calculation of the magnetic field of a nerve action potential. Biophysics Journal 32:719–732.

Troung, T.K. & A.W. Song. 2006. Finding neuroelectric activity under magnetic field oscillations (NAMO) with magnetic resonance imaging in vivo. Proceedings of the National Academy of Science USA 103:12598–12601.

van Egeraat, J.M., R.N. Friedman & J.P. Wikswo. 1990. Magnetic field of a single muscle fiber: First measurement and a core conductor model. Biophysics Journal 57:663–667.

van Egeraat, J.M. & J.P. Wikswo. 1993. A model for axonal propagation incorporating both radial and axial ionic transport. Biophysics Journal 64:1287–1298.

van Egeraat, J.M., R. Stasaski, J.P. Barach, R.N. Friedman & J.P. Wikswo. 1993. The biomagnetic signature of a crushed axon: A comparison of theory and experiment. Biophysics Journal 64: 1299–1305.

Wijesinghe, R.S., F.L.H. Gielen & J.P. Wikswo. 1991. A model for compound action potentials and currents in a nerve bundle III: A comparison of the conduction velocity distributions calculated from compound action currents and potentials. Annals of Biomedical Engineering 18:97–121.

Wijesinghe, R.S. & B.J. Roth. 2009. Detection of Peripheral Nerve and Skeletal Muscle Action Currents Using Magnetic Resonance Imaging. Annals of Biomedical Engineering 37(11):2402–2406.

Wikswo, J.P. & J.M. van Egeraat. 1991. Cellular magnetic fields: Fundamental and applied measurements on nerve axons, peripheral nerve bundles, and skeletal muscle. Journal of Clinical Neurophysiology 8:170–188.

Wikswo, J.P., J.P. Barach & J.A. Freeman. 1980. Magnetic field of a nerve impulse: First measurements. Science 208:53–55.

Wikswo, J.P., W.P. Henry, R.N. Freidman, W.A. Kilroy, R.S. Wijesinghe, J.M. van Egeraat, M.A. Milek. 1990. Intraoperative recording of the magnetic field of a human nerve. Pp. 137–140. *In* Advances in Biomedicine. (S.J. Williamson, M. Hoke, G. Stroink & M. Kotani). Plenum, New York.

Woosley, J.K., B.J. Roth & J.P. Wikswo. 1985. The magnetic field of a single axon: A volume conductor model. Mathematical Biosciences 76:1–36.

Xue, X., X. Chen, T. Grabowski & J. Xiong. 2009. Direct MRI mapping of neuronal activity evoked by electrical stimulation of the median nerve at the right wrist. Magnetic Resonance in Medicine 61:1073–1082.

Manuscript received 20 June 2011, revised 16 January 2012.